Progress in Physics of Applied Materials 2 (2022) 157–164

Semnan University

Progress in Physics of Applied Materials

journal homepage: https://ppam.semnan.ac.ir/

Effect of Electric Field Magnitude on the Mechanical Behavior of Silicon-Doped Nanoporous Carbon Matrix by Molecular Dynamics Method

M. Hekmatifar[1*], D. Toghraie[1], R, Sabetvand[2], S. Esmaeili[1]

[1]*Department of Mechanical Engineering, Khomeinishahr Branch, Islamic Azad University, Khomeinishahr, Iran*
[2] *Department of Energy Engineering and Physics, Faculty of Condensed Matter Physics, Amirkabir University of Technology, Tehran, Iran*

ARTICLE INFO

Article history:
Received: 22 November 2022
Revised: 18 December 2022
Accepted: 24 December 2022

Keywords:
Silicon Doping
Carbon Matrix
Molecular Dynamics simulation
Young's Modulus

ABSTRACT

Porous materials are a new category of materials which have attracted the attention of scientists and different industries due to their special mechanical properties (MP), such as definable strength and density. This research aims to study the effects of an electric field on the MP of a silicon nanoparticle (NP)-doped carbon matrix with 10% porosity. MP studied in this research include Young's modulus (YM), and ultimate strength (US), obtained using the molecular dynamics (MD) simulation method and LAMMPS comprehensive software. The results show that the US and YM of silicon-doped nanoporous carbon matrix converged to 69.4014 GPa and 200.192GPa, respectively. In the following, the mechanical strength in simulated samples decreases by increasing the electric field magnitude. Numerically, by increasing the electric field from 0.2 to 0.5 V/Å, the US and YM of silicon-doped nanoporous carbon matrix decreased from 65.83 and 191.022 GPa to 57.81, and 167.18 GPa.

1. Introduction

Porosity is obtained by dividing the volume of pores by the total volume of material. Porous materials attracted the attention of scientists in terms of various applications in the molecular separation, heterogeneous catalysis, absorption technology or light, and electronics technology. In general, the surface area of a porous material is higher than that of its non-porous material. The holes in porous materials are divided into open holes and closed holes. Open holes have the accessibility to the material's surface, but closed holes are trapped inside the material [1-3]. Porous materials are identified in terms of the pore size obtained from gas absorption data. In 1985, International Union of Pure and Applied Chemistry classified pore sizes as follows [4]. The first category includes the microporous materials. The size of pores in these materials is smaller than 2 nm. The second category includes the mesoporous materials, the pore size of these materials is from 2 to 50 nm, and the third includes the macroporous materials. The pore size of these materials is larger than 50 nm [5-7]. The functions of three categories of the mentioned pores are different from each other. Micropores have a large SSA, the mesopores increase mass transfer in terms of low mass transfer resistance, and macropores have rich and large reactive reservoirs which makes the mass transfer paths shorter. Hierarchical pores increase the access of the reactants to the micropores, leading to an increase in the reaction rate. Hierarchical porous carbons have excellent performance in applications which include energy storage, catalysis, and adsorption [8-10]. Many studies investigated the properties and different applications of hierarchically porous carbon materials [11-14]. The results of researchers showed that the porous carbon materials have weak stability and strength. To overcome this challenge, we can use the method of doping these materials with nano materials. One of the materials used in this method was silicon NPs [15]. Silicon NPs were environmentally friendly which could be easily doped with the organic molecules. Besides, silicon NPs have good resistance to wear, to wear and pressure [16]. Studies on using silicon doping were conducted by researchers [17-20]. Chaus et al.[21] improved the MP of

* Corresponding author.
E-mail address: maboud.hekmatifar@iaukhsh.ac.ir

DOI: 10.22075/ppam.2022.29073.1045

amorphous carbon layers with the silicon doping. The results show that doping amorphous carbon layers with the silicon reduced the residual stresses and surface energy and affected the friction coefficient. The properties of amorphous carbon films doped with silicon depended on silicon concentration. Sikora et al.[22] investigated the mechanical properties of carbon nanotube-silica. The results showed that adding 0.125 %wt of silica NPs improved the MP of carbon nanotubes. Fu et al.[23] investigated the MP of GO/SiO_2 multilayers films on carbon fibers. The results showed that the tensile strength increased from 3.52 GPa to 3.68 GPa after adding GO/SiO_2. Divya et al.[24] investigated the effect of adding SiO_2 NP on MP of carbon fabric reinforced epoxy. The results show that adding SiO_2 NPs improved the MP of epoxy. The researchers' results show that the addition of external force, including the magnetic and electric fields, affected the MP of materials[25]. For example, Gao et al.[26] investigated the effect of electric field on MP of carbon nanotubes. The results showed that the addition of an electric field had an effect on the MP.

In recent years, using the computer simulation methods had received much attention in terms of saving time and money[27]. One of the methods used was MD simulation. MD was a method to simulate the thermodynamic behavior of materials in three phases of solid, liquid, and gas using force, velocity, and the location of particles[28]. The main goal in MD simulation was to calculate the macroscopic behavior of a system by helping a microscopic model. A model which included the mechanical interaction among the molecules. Statistical mechanics provided a suitable theoretical tool for MD simulation[29]. Han et al. [30] used the MD simulations to study the MP of graphene sheets doped with silicon, nitrogen or base atoms. YM, ultimate stress (strain), and energy absorption were studied for graphene sheets with 0 to 5% doping concentrations. The results show that incorporating impurities in graphene led to a linear decrease in YM. Rahman et al. [31] investigated the MP and fracture phenomenon of graphene doped with silicon by the MD simulation. The results showed that the graphene's fracture stress, and fracture strain decreased significantly by increasing silicon concentration. The YM of graphene decreased by 15.5% in the armchair direction and 13.5% along with the zigzag direction using 5% silicon doping. Zhao et al.[32] investigated the effect of SiO_2 addition on MP of graphene by MD simulation. The results showed that the MP of graphene were low and improved by adding SiO_2. Wei et al.[33] investigated the effect of SiO_2 addition on MP of polypropylene by the MD simulation. The results showed that doping was a suitable method to improve MP.

Based on previous research, the effects of electric field on the MP of silicon-doped carbon matrix have not been studied so far. For this reason, the effects of electric field on MP, such as stress-strain curve, YM, and US of porous carbon matrix with 10% porosity were analyzed. Moreover, the MD simulation and LAMMPS software were used, and the results were analyzed.

2. The MD simulation approach

The MD approach is a form of computer simulation in which the atoms and molecules are allowed to interact for a period under the known laws of physics to give an insight into the motion of atoms. In the MD simulation, the real dynamic behavior of system was calculated, which could be used to calculate the time average of system's properties. Using this method, the system's state in any future time can be predicted from its current state. In this method, Newton's equations of motion were integrated by breaking the calculation into a set of short time steps (fs, ps, and ns). In each step, the forces on the atoms were calculated and combined with the current positions and velocities to obtain new positions and velocities quickly ahead. The second law of Newton directly related the motion to applied force as follows [34]:

$$F_i = m_i a_i = -\nabla_i U = -\frac{dU}{dr_i} \tag{1}$$

F_i is the force applied to the particle, m_i and a_i are the mass and the acceleration of particle, and resources r_i is the particle's position relative to a fixed reference frame. Since the force applied on a particle depends on the position of that particle relative to the others and in terms of the paired nature of particle motion, the analytical description of particle motion was difficult. Hence, the integration of the equations of motion was done by numerical methods; hence, Verlet algorithm was introduced efficiently [35, 36]. The MD method solves Newton's equations of motion for atoms by considering small time steps and predicts atoms' new positions and velocities in each step using approximate numerical methods. At new positions, the atomic forces are recalculated, and the next time step is created. In a simulation, this process was repeated thousands of times. An integral algorithm was the approximate numerical method to advance the system by a one-time step. The velocity-Verlet algorithm produced the position and velocity of particles at the moment in time which was known as the complete algorithm in this sense. Position (r_i), velocities (v_i) and accelerations in time were obtained from the corresponding values of these quantities in time t as follows [37-39]:

$$r_i\left(\mathrm{t}+\ \Delta\mathrm{t}\right) = 2\ r_i\left(t\right) - r_i\left(t-\Delta t\right) + \left(\frac{d^2 r_i}{dt^2}\right)\left(\Delta t\right)^2 \tag{2}$$

$$v_i\left(t+\Delta t\right) = v_i\left(t\right) + \Delta t\, a_i\left(t\right) + \frac{\Delta t\left(a_i\left(t\right)+a_i\left(t+\Delta t\right)\right)}{2} \tag{3}$$

$$a_i\left(t+\Delta t\right) = \frac{F_i\left(t+\Delta t\right)}{m_i} \tag{4}$$

One of the important factors in the MD simulation method was the definition of potential function and interparticle forces. In other words, the MD simulation required the definition of a potential function that provided a complete description of the interaction among the particles. The present research used the Tersoff potential function to determine the interaction among the carbon

atoms in studied structure. Tersoff potential function was described using following mathematical function [40, 41]:

$$E = \frac{1}{2}\sum_{i}\sum_{j\neq i} U_{ij} \tag{5}$$

$$U_{ij} = f_C\left(r_{ij}\right)\left[a_{ij} f_R\left(r_{ij}\right) + b_{ij} f_A\left(r_{ij}\right)\right] \tag{6}$$

$$f_C(r) = \begin{cases} 1 & r < R - D \\ \frac{1}{2} - \frac{1}{2}\sin\left(\frac{\pi}{2}\frac{r-R}{D}\right) & R - D < r < R + D \\ 0 & r > R + D \end{cases} \tag{7}$$

In Eq. (6), f_R is the attraction particle interaction with the general form as follows:

$$f_R(r) = A\exp(-\lambda_1 r) \tag{8}$$

and f_A is the particle-repellent interaction with the general form as follows:

$$f_A(r) = -B\exp(-\lambda_2 r) \tag{9}$$

In above equations, A, B, and are the potential constants which are dependent on studied structures. Furthermore, b_{ij} defined in Eq.6 is determined as follows:

$$b_{ij} = \left(1 + \beta^n \varphi_{ij}{}^n\right)^{-\frac{1}{2n}} \tag{10}$$

$$\varphi_{ij} = \sum_{k\neq ij} f_C(r_{ik}) g(\theta_{ijk}) exp[\lambda_3^m \left(r_{ij} - r_{ik}\right)^m] \tag{11}$$

The function of g(θ) is related to the angle between i and j particles and between i and k particles.

2.1 The MD simulation details

At first, the silicon-doped nanoporous carbon matrix (with 10% porous) was modelled with Avogadro software. The pores were created by removing the atoms from circular areas of various diameters in nanoporous carbon matrix. Figure 1 shows the schematic of simulated silicon-doped nanoporous carbon matrix. The length of simulation box was 40 nm, and the boundary condition was periodic in all directions. The initial pressure and temperature were set to 0 bar and 300 K using NPT ensemble. The equilibration in the matrix was evaluated with the change in temperature and kinetic energy. In the final step, the MP of simulated matrix were calculated. By increasing the electric field from 0.1 to 0.5 V/Å, the change in MP of the simulated matrix was calculated. Under the electric field, the charge distribution in a structure will be changed because of electric polarization so that the tube is not electrically neutral. This in turn will cause the structure to be stretched by the electric field.

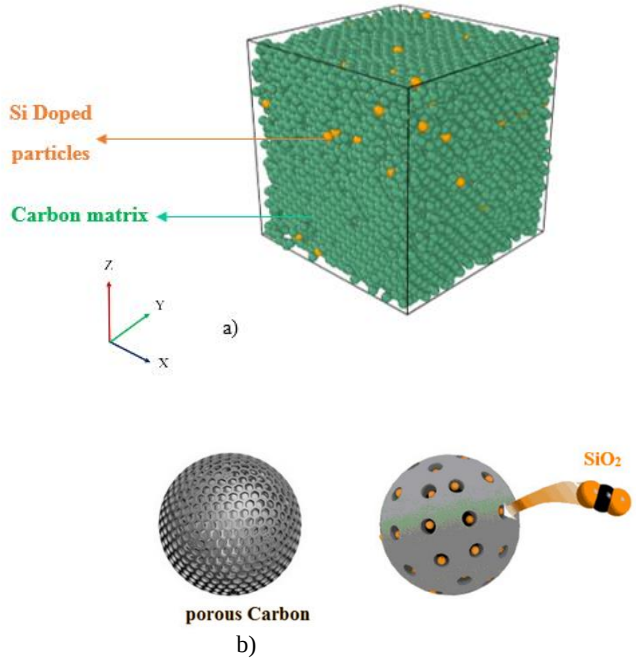

3. Fig.1. A schematic of simulated silicon-doped nanoporous carbon matrix from.

The silicon-doped nanoporous carbon matrix was stretched along with X-axis with a tensile loading (with 0.01 ps magnitude) from both sides to examine MP. Figure 2 shows a schematic of the mechanical test of silicon-doped nanoporous carbon matrix.

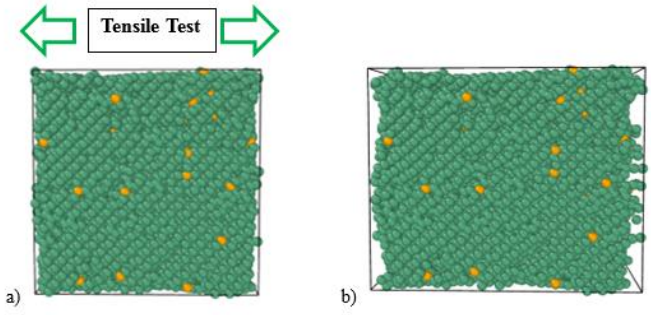

Fig.2. A schematic of tensile test at a) first and b) after 200,000-time steps.

2.2. Equilibrium of the structure

This study's results were divided into two stages. In other words, before determining the MP of silicon-doped nanoporous carbon matrix, the physical quantities, such as temperature and kinetic energy were studied to create equilibrium and determine the atomic behavior of desired

structure. In the next step, the results of the MP of desired carbon matrix were reported. Equilibrium in atomic samples was very important based on defined initial conditions. The equilibrium duration in the desired structure equaled 100,000 time steps. Figure 3 indicates the temperature changes in the studied nanostructure to the simulation time. Based on the results of Figure 3, the temperature value of the simulated structure converged at 300 K after 100,000-time steps. Time step selection depends on what structural interactions we want to probe, e.g., H-bonding, confrontational change, binding interaction, etc., each of which has its time scale of existence. It is not much dependent on the system size (box size). Still, it depends on the size of molecule if going to study the conformation changes of large proteins or other biomacromolecules (the time scale for such a process may vary from less than a ns to a few seconds). This thermodynamic behavior shows the reduction of temperature fluctuations over time. In other words, reducing the oscillation range of the silicon-doped nanoporous carbon matrix atoms studied in the simulation box reduced particle mobility. This issue caused the temperature equilibrium of final structure and thus, the stability of overall atomic structure. It indicates the stability of atomic samples, which resulted from the simulation settings, such as the correct choice of potential function in LAMMPS simulation input code.

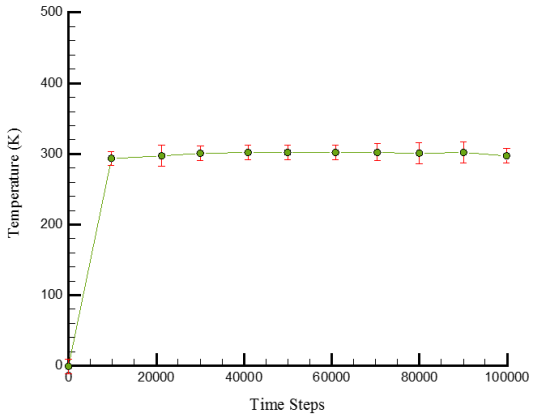

Fig. 3. Temperature variations vs time steps.

Based on the results presented in the previous section, the temperature of desired nanostructure was proportional to the movement and fluctuations of atoms. Therefore, the kinetic energy will converge in the nanostructure in terms of temperature convergence. Convergence in the numerical value of kinetic energy in the structure under study occurred to more prominent attraction energy than repulsion energy, which led to convergence in atomic motions and, at last, merging esteem of the individual particle's interior of simulation box. Therefore, the amount of kinetic energy converged to a specified amount based on temperature variations. Figure 4 illustrates the changes in the studied nanostructure's kinetic energy against the simulation time. Numerically, the kinetic energy of studied nanostructure converged to 758.17 eV after 100,000 time steps. The convergence shown in Figure 4 led to the reduction of fluctuations in this nanostructure. Therefore, considered nanostructure had a suitable thermodynamic and temperature equilibrium and showed the proper definition of atomic nanostructures and interatomic potential. Because it led to the stability in the inter-atomic distance of NPs, the kinetic energy of atomic samples had subsequently approached a certain value.

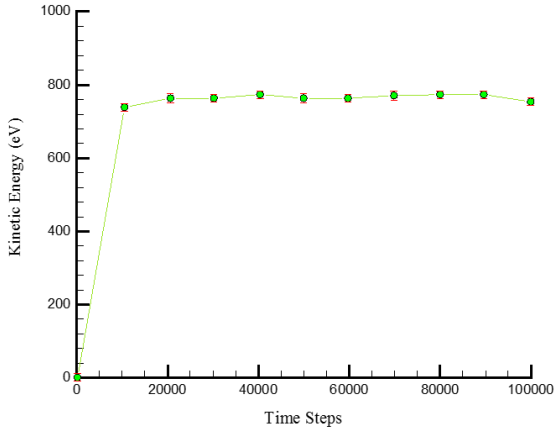

Fig.4. Kinetic energy variations vs simulation time.

3. Results and discussion

In general, an electric field entered the charged particles. Applying the field caused the movement of charged particles and, therefore, could affect the atomic and mechanical behavior of the studied structure. Figure 5 shows the change in the stress-strain curve. The results show that the final strength of the simulated structure was equal to 69.4014 GPa. The simulation results were consistent with the results of Zhao et al.[32]. The results of Zhao et al.[32] showed that the US of porous graphene with SiO_2 was equal to 75 GPa.

The slope of stress-strain diagram showed YM. Figure 5 (b) shows the YM of the simulated silicon-doped nanoporous carbon matrix in an electric field with 0.1 V/Å. The numerical results show that the YM of silicon-doped nanoporous carbon matrix converged to 200.192GPa. The obtained results are reported in Table 1.

3.1. The effect of electric field

Increasing the electric field makes it possible to create oscillations and increase the kinetic energy in the simulated structure. Therefore, the interaction among particles decreased and the stability of studied structure decreased. Therefore, it is expected that the mechanical strength in the structure will decrease by increasing the electric field. Figure 6 shows the change in the stress-strain curve and YM of the simulated silicon-doped nanoporous carbon matrix by increasing electric field. The obtained results show that by increasing an electric field, the mechanical strength in the simulated silicon-doped nanoporous carbon matrix was reduced. The research was consistent with that of Guo et al.[42]. Guo et al. [42] investigated the effect of electric field on the MP of carbon

nanotubes. Their results showed that by adding an electric field, the MP, including the YM, decreased.

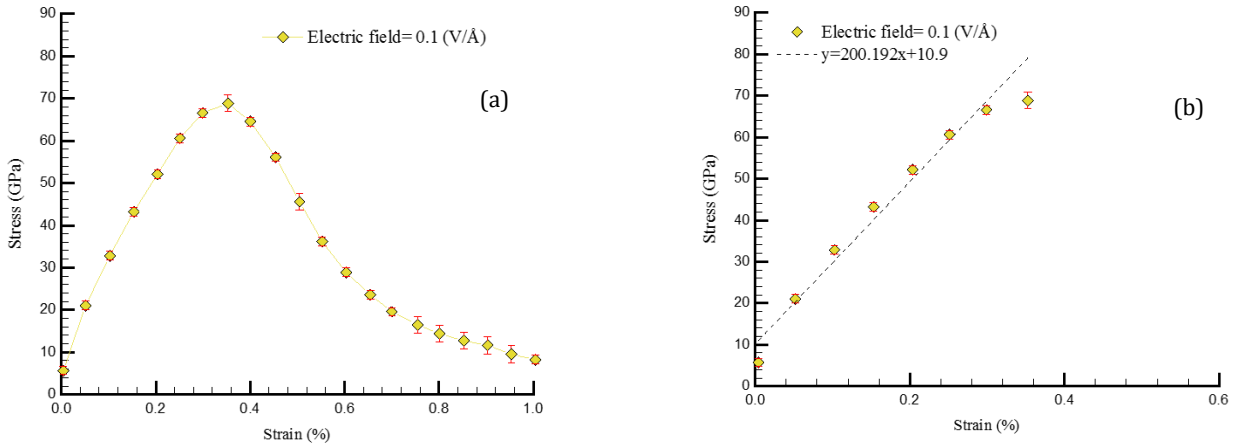

Fig. 5. a) stress-strain curve and b) YM of simulated silicon-doped nanoporous carbon matrix

The change in the US and YM of silicon-doped nanoporous carbon matrix by increasing the electric field are shown in Figures 7 and 8. Numerically, by increasing the electric field from 0.2 to 0.5 V/Å, the US and YM of silicon-doped nanoporous carbon matrix decreased from 65.83 and 191.022 GPa to 57.81 and 167.18 GPa. As electric field increased, the polarity of molecules increased and created strong repulsion among the atoms. Consequently, the distance among the atoms increased. As the distance among the atoms increased, the bands become weaker and cause the MP to decrease.

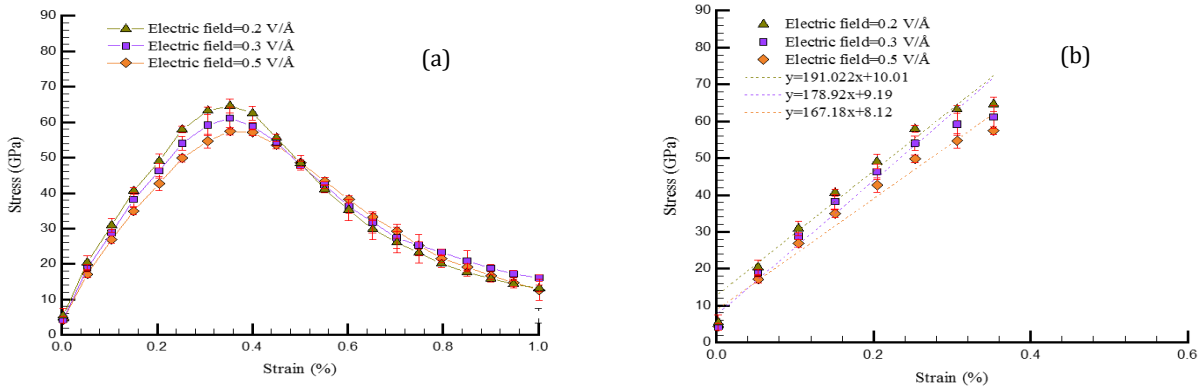

Fig.6. a) The stress-strain curve and b) YM of simulated silicon-doped nanoporous carbon matrix with increasing electric field.

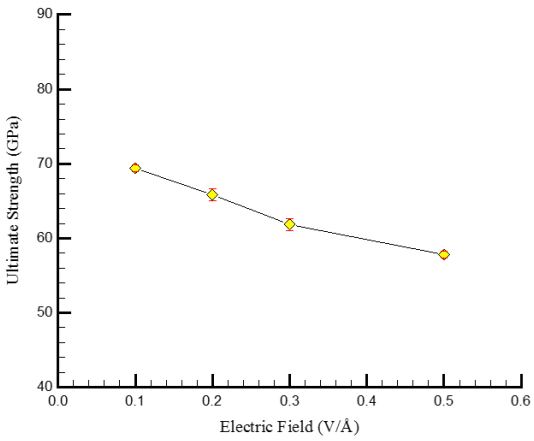

Fig. 7. Change in the US of simulated silicon-doped nanoporous carbon matrix with increasing electric field.

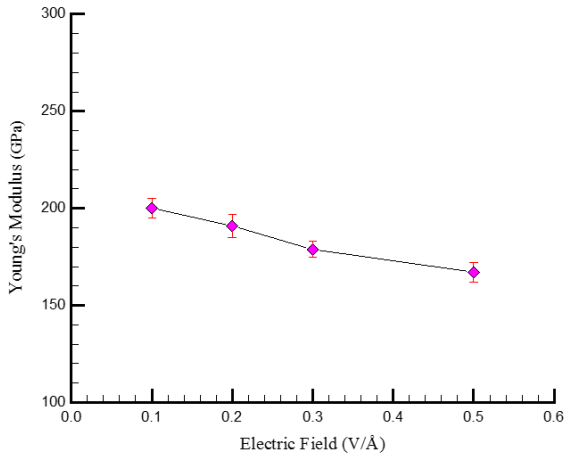

Fig. 8. Change in YM of simulated silicon-doped nanoporous carbon matrix by increasing electric field.

Table 1. Changes in US and YM of the simulated matrix with increasing electric field.

Electric field (V/Å)	US (GPa)	YM (GPa)
0.1	69.4014	200.192
0.2	65.83	191.022
0.3	61.84	178.92
0.5	57.81	167.18

4. Conclusion

In summary, the effect of electric field on the MP of silicon-doped nanoporous carbon matrix was studied. This study was done by the MD simulation. The study of the MP of studied structure was done based on the change of stress-strain diagram and the calculation of YM and US. The nets of the most important results obtained are expressed as follows:

- The simulated structure's temperature and kinetic energy value converged at 300 K after and 758.17 eV after 100,000-time steps. This convergence indicated the stability of atomic samples, which resulted from the simulation settings, such as the correct choice of potential function in the LAMMPS simulation input code.
- The US and YM of silicon-doped nanoporous carbon matrix converged to 69.4014 GPa and 200.192GPa, respectively, in the presence of an electric field with 0.1 V/Å magnitudes.
- By increasing an electric field, the mechanical strength in the simulated silicon-doped nanoporous carbon matrix was reduced. This reduction was in terms of the increase in the kinetic energy and fluctuations in the simulated matrix by increasing the electric field.
- Numerically, by increasing the electric field from 0.1 to 0.5 V/Å, the US and YM of silicon-doped nanoporous carbon matrix decreased to 57.81 and 167.18GPa.

References

[1] K. Kaneko, "Determination of pore size and pore size distribution: 1. Adsorbents and catalysts." Journal of membrane science 96 (1994) 59-89.

[2] D. M. Antonelli, J. Y. Ying, "Mesoporous materials." Current Opinion in Colloid & Interface Science 1 (1996) 523-529.

[3] K. Ajay, M. Dinesh, G. Byatarayappa, M. Radhika, N. Kathyayini, H. Vijeth, "Electrochemical investigations on low cost KOH activated carbon derived from orange-peel and polyaniline for hybrid supercapacitors." Inorganic Chemistry Communications 127 (2021) 108523.

[4] T. Mays, "A new classification of pore sizes." Characterization of Porous Solids 160 (2007) 57-62.

[5] B. Li, H. Xiong, and Y. Xiao, "Progress on synthesis and applications of porous carbon materials." Int. J. Electrochem. Sci 15 (2020) 1363-1377.

[6] T. Kesavan, T. Partheeban, M. Vivekanantha, M. Kundu, G. Maduraiveeran, M. Sasidharan, "Hierarchical nanoporous activated carbon as potential electrode materials for high performance electrochemical supercapacitor." Microporous and Mesoporous Materials 274 (2019) 236-244.

[7] S. De, A. M. Balu, J. C. Van Der Waal, R. Luque,"Biomass-derived porous carbon materials: synthesis and catalytic applications." ChemCatChem 7 (2015) 1608-1629.

[8] X.-L. Zhou, H. Zhang, L.-M. Shao, F. Lü, P. J. He, "Preparation application of hierarchical porous carbon materials from waste biomass: A review." Waste and Biomass Valorization 12 (2021) 1699-1724.

[9] B. Chang, Y. Guo, Y. Li, H. Yin, S. Zhang, B. Yang, X. Dong, "Graphitized hierarchical porous carbon nanospheres: simultaneous activation/graphitization and superior supercapacitance performance." Journal of Materials Chemistry 3 (2015) 9565-9577.

[10] Y.T. Li, Y.T. Pi, L.M. Lu, S.H. Xu, T.Z. Ren, "Hierarchical porous active carbon from fallen leaves by synergy of K_2CO_3 and their supercapacitor performance." Journal of Power Sources 299 (2015) 519-528.

[11] L. Wang, X. Hu, "Recent advances in porous carbon materials for electrochemical energy storage." Chemistry–An Asian Journal 13 (2018) 1518-1529.

[12] B. Li, H. Xiong, Y. Xiao, "Progress on synthesis and applications of porous carbon materials." Int. J. Electrochem. Sci 15 (2020) 1363-1377

[13] J. Lee, J. Kim, T. Hyeon, "Recent progress in the synthesis of porous carbon materials." Advanced materials 18 (2006) 2073-2094.

[14] X. Yang, C. Li, Y. Chen, "Hierarchical porous carbon with ultrahigh surface area from corn leaf for high-performance supercapacitors application." Journal of Physics D: Applied Physics 50 (2017) 055501.

[15] F. Xu, G. Nava, P. Biswas, I. Dulalia, H. Wang, Z. Alibay, M. Gale, D. J. Kline, B. Wagner, L. Mangolini, "Energetic characteristics of hydrogenated amorphous silicon nanoparticles." Chemical Engineering Journal 430 (2022) 133140.

[16] M. Vallet-Regí, "Our contributions to applications of mesoporous silica nanoparticles." Acta Biomaterialia 137 (2022) 44-52.

[17] A. R. Albooyeh, A. Dadrasi, A. H. Mashhadzadeh, "Effect of point defects and low-density carbon-doped on mechanical properties of BNNTs: A molecular dynamics study." Materials Chemistry and Physics 239 (2020) 122107.

[18] L. Zhang, M. Kai, X. Chen, "Si-doped graphene in geopolymer: Its interfacial chemical bonding, structure evolution and ultrastrong reinforcing ability." Cement and Concrete Composites 109 (2020) 103522.

[19] J.I. Kim, Y.J. Jang, J. Kim, J. Kim, "Effects of silicon doping on low-friction and high-hardness diamond-like carbon coating via filtered cathodic vacuum arc deposition." Scientific reports 11 (2021) 1-13.

[20] R. Zarei Moghadam, H. Rezagholipour Dizaji, M. Ehsani, "Modification of optical and mechanical properties of nitrogen doped diamond-like carbon layers." Journal of Materials Science: Materials in Electronics 30 (2019) 19770-19781.

[21] A. S. Chaus, X. H. Jiang, P. Pokorný, D. G. Piliptsou, A. V. Rogachev, "Improving the mechanical property of amorphous carbon films by silicon doping. " Diamond and Related Materials 82 (2018) 137-142.

[22] P. Sikora, M. Abd Elrahman, S.Y. Chung, K. Cendrowski, E. Mijowska, D. Stephan, "Mechanical and microstructural properties of cement pastes containing carbon nanotubes and carbon nanotube-silica core-shell structures, exposed to elevated temperature." Cement and Concrete Composites 95 (2019)193-204.

[23] J. Fu, M. Zhang, L. Jin, L. Liu, N. Li, L. Shang, M. Li, L. Xiao, Y. Ao, "Enhancing interfacial properties of carbon fibers reinforced epoxy composites via Layer-by-Layer self assembly GO/SiO_2 multilayers films on carbon fibers surface." Applied Surface Science 470 (2019) 543-554.

[24] G. Divya, B. Suresha, "Impact of nano-silicon dioxide on mechanical properties of carbon fabric reinforced epoxy composites." Materials Today: Proceedings 46 (2021) 8999-9003.

[25] J. Roche, "Introducing electric fields." Physics Education 51 (2016) 055005.

[26] J. Gao, Y. He, X. Gong, "Effect of electric field induced alignment and dispersion of functionalized carbon nanotubes on properties of natural rubber." Results in Physics 9 (2018) 493-499.

[27] M. P. Allen, D. J. Tildesley, "Computer simulation of liquids." Oxford university press (2017).

[28] T. Hansson, C. Oostenbrink, W. van Gunsteren, "Molecular dynamics simulations." Current opinion in structural biology 12 (2002) 190-196.

[29] J. M. Haile, "Molecular dynamics simulation: elementary methods." John Wiley & Sons, Inc. (1992).

[30] T. Han, Y. Luo, C. Wang, "Effects of SI, N and B doping on the mechanical properties of graphene sheets." Acta Mechanica Solida Sinica 28 (2015) 618-625.

[31] M. H. Rahman, S. Mitra, M. Motalab, P. Bose, "Investigation on the mechanical properties and fracture phenomenon of silicon doped graphene by molecular dynamics simulation." RSC advances 10 (2020) 31318-31332.

[32] Y. Zhao, G. Xie, J. Zhao, C. Wang, C. Tang, "Modifying mechanical properties of silicon dioxide using porous graphene: molecular dynamics simulations." Materials Research Express 8 (2021) 055012.

[33] S. Wei, X. Li, Y. Shen, L. Zhang, X. Wu, "Study on microscopic mechanism of nano-silicon dioxide for improving mechanical properties of polypropylene." Molecular Simulation 46 (2020) 468-475.

[34] B.J. Alder, T.E. Wainwright, "Studies in molecular dynamics. I. General method." The Journal of Chemical Physics 31 (1959) 459-466.

[35] W. C. Swope, H. C. Andersen, P. H. Berens, K. R. Wilson, "A computer simulation method for the calculation of equilibrium constants for the formation of physical clusters of molecules: Application to small water clusters." The Journal of chemical physics 76 (1982) 637-649.

[36] E. Hairer, C. Lubich, G. Wanner, "Geometric numerical integration illustrated by the Störmer–Verlet method." Acta numerica 12 (2003) 399-450.

[37] L. Verlet, "Computer "experiments" on classical fluids. I. Thermodynamical properties of Lennard-Jones molecules." Physical review 159 (1967) 98.

[38] W. C. Swope, H. C. Andersen, P. H. Berens, K. R. Wilson, "A computer simulation method for the calculation of equilibrium constants for the formation of physical clusters of molecules: Application to small water clusters." The Journal of chemical physics 76 (1982) 637-649.

[39] E. Hairer, C. Lubich, G. Wanner, "Geometric numerical integration illustrated by the Störmer–Verlet method." Acta numerica 12 (2003) 399-450.

[40] J. Tersoff, "Empirical interatomic potential for silicon with improved elastic properties." Physical Review B 38 (1988) 9902.

[41] J. Tersoff, "Empirical interatomic potential for carbon, with applications to amorphous carbon." Physical Review Letters 61 (1988) 2879.

[42] Y. Guo, W. Guo, "Mechanical and electrostatic properties of carbon nanotubes under tensile loading and electric field." Journal of physics D: Applied physics 36 (2003) 805.